University of Thi-Qar Journal for Engineering Sciences
Volume 16, Issue 1, June 2026
https://doi.org/10.32792/utq/utjes.16.1.745

Analysis of Optical Received Power in the VLC System

Huda Anwar [1]

Received:26th January 2026/Accepted: 30th March 2026/ Published Online: 1st June 2026

Abstract

As the growth of the requirement towards Sixth Generation 6G desirable for advanced technologies to offer extreme performance and facilities, this makes Visible Light Communication (VLC) one of the greatest nominees. This paper estimates the performance of VLC in line-of-sight (LOS) and Non-line-of-sight (NLOS) environments. Investigate the effect of distance and various transmission angle adjustments on the received power and signal-to-noise ratio (SNR) from the transmitter side. Furthermore, from the receiver side, the impact of the optical concentrator gain with distance is studied. The contour plot for both the received power and SNR is studied to present the maximum power according to the effect of the considered parameters. The results show that a high amount of the received power can be achieved with high values of irradiance angle, especially in small distances. For SNR, the maximum value is evaluated at low values for both distance and irradiance angle under the effect of high Lambertian order in the LOS case. In NLOS, a general reduction is notable, especially at large distances. From the receiver perspective, the results show that large values for the received power and SNR are evaluated as the values of the concentrator gain are increased. Also, the optical filter influence on received power and SNR has been studied.

Keywords—Visible Light Communications, Received power, Field of View, Optical Filter, Concentrator Gain

1 Introduction

In the new era of highly dependent environments on the internet and various technologies that require safe communication and high data broadcasting, this places a burden the excited systems and techniques. Many of the challenges still being addressed in Fifth Generation (5G) can be managed in easier, better, or more effective ways using various approaches such as millimeter wave (Zhou et al., 2025), Tera-hertz, and Visible Light Communication (VLC) (Ariyanti & Suryanegara, 2020; He & Chen, 2023). VLC is a virtual section of optical communication that depends on exploiting the range of the spectrum of visible light (Chowdhury et al., 2025). Many fields adopt VLC in their systems to capture the benefit, including underwater (Jayaweera et al., 2025), medical (Antaki et al., 2025), and IoT (Batista et al., 2025). Recently, in the VLC system, a lot of aspects have been under consideration to research the performance of the system to meet the expectations of the next generation, such as Optical Orthogonal Frequency Multiple Access (Jaque Intriago et al., 2025) and vehicle-to-vehicle in the VLC system (Al Hasnawi et al., 2025). One of the features that highlighted in this research is the signal alignment and distance. VLC extremely depends on different angles and parameters to enhance the performance. In the VLC system, the transmitter side has a lot of influence on the amount of power conveyed to the receiver. The basic components of the VLC receiver are: Photodiode, Filter (an optical type), and Concentrator (He & Chen, 2023). The optical filter, similar in idea to general filtering, permits only a partial wavelength of the light signal to pass and blocks any other wavelengths that may be related to noise. Researchers in (Abdalla et al., 2020; Abualhoul et al., 2014; Nagaraja et al., 2025) consider the effect of the Field

Huda Anwar
huda@utq.edu.iq
[1] Department of Electrical and Electronics engineering, College of Engineering, University of Thi-Qar, Thi-Qar, Iraq

of View (FoV) from their perspective. In (Abdalla et al., 2020), the authors show the impact of variable values of FoV in a concentrated environment on the performance, considering SNR as a performance metric. The results show the benefit of using adaptive values to decrease the interference. Also, in (Al-Sakkaf & Morales-Céspedes, 2024), the authors show that by using different FoV values, incorporate in alleviate interference between different adjacent recovers. In (Eroğlu et al., 2018), the effect of FoV in the case of single and multiple LEDs is presented. They rely on probability distribution for the channel to perform their simulation as it is the basic for calculating bit error rate (BER). Their investigation shows that better results are obtained with a wider FoV angle and more transmitter LEDs. On the other side, authors in (Putri et al., 2019) present the system performance for different modulation types. Their researcher considers BER as the performance metric to study the effectiveness of the concentrator gain of the VLC system in an LOS environment. Authors in (Saxena et al., 2018) show an optimization method to get the appropriate semi-angle value that attains the maximum value for the receiver power. Their results show that for a specific number of LEDs, there is an optimal value for semi-angle that provides a suitable level of power. As the VLC system has a lot of applications, Eso et al., 2021 investigated the BER performance for a system combining a vehicular link with a relay. As part of their work, they show the effect of the incidence angle in case the cars are not on the same line, which causes a modification in the incidence angle. Their results show that a drop in BER for a specific value of incident angle may be overcome by increasing the area of the photodiode. These studies show the significant importance of geometric factors and receiver optical features. The contribution of this work is:

1. Studying the performance of the system from both sides, the transmitter and receiver, combining the effect of angles from each side with the distance variation for both sides to capture the whole impact on the received power.
2. This paper investigates the impact of concentrator gain on the receiver optical power.
3. This paper studies the impact of different values of the optical filter.
4. Performance comparison for the system in LOS and NLOS environments.

In addition, the contour plot for the received power and SNR is evaluated to show the distribution of the power in a more efficient manner. The paper organizes in the following sections: Section 2 presents the mathematical model for our considered system, followed by Section 3, which discusses the simulation results, Finally the conclusion of the paper.

2 Mathematical Model

The VLC system consists of three essential parts: a transmitter, an optical wireless channel, and a receiver. In this paper, LOS and NLOS are assumed between the transmitter and receiver as presented in Figure 1. The data signal is converted to an optical signal on the transmitter side and emitted to the receiver with a Lambertian pattern. The Lambertian pattern explores the spreading of the power depending on the semi-angle, in which the light intensity is related to the cosine of this angle from where the light is radiating (Ding et al., 2019; Zhou et al., 2025). In the LOS part of the VLC system, the signal radiation is similar to the Lambertian pattern model (that depend on cosine) with an order ***m*** called the Lambertian order, given as (Poulose, 2022)

$$m = -\frac{\ln(2)}{\ln\left(\cos\left(\varphi_{\frac{1}{2}}\right)\right)} \tag{1}$$

The semi-angle of the half-power value is denoted as $\varphi_{1/2}$. The signal travels at an angle ϕ from the transmitter through an optical channel to the receiver. The signal incidents to the receiver at an angle ψ. This reflected on the channel for LOS, as in (De Oliveira et al., 2022)

$$H_{LoS} = \frac{(m+1)\,A}{2\pi d^2} cos^m(\phi)T(\psi)g(\psi)\cos(\psi) \quad (2)$$

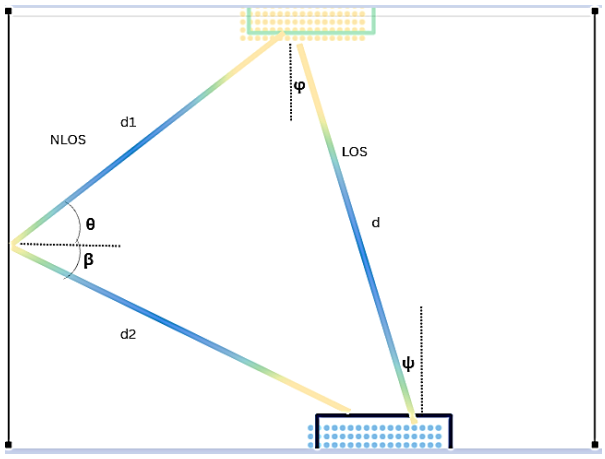

Figure 1: Proposed VLC system

The effective area of the photodetector is represented as A, ϕ is the irradiance angle enclosed between the normal of the transmitter and the line between the transmitter to receiver, ψ is the angle related to the receiver, d is the distance from the transmitter to the receiver, and $T(\psi)$ characterizes filter gain.

The receiver parameter has a critical impact on the VLC system. The receiver contains: a filter, a concentrator and a photodetector. The Concentrator has a factor known as the concentrator gain $g(\psi)$ that raises the amount of power on the photodiode for a specific incident angle ψ_r. On the receiver side, where the concentrator excites, the gain is given (Farfán–Guillén et al., 2021; Raj et al., 2020):

$$(\psi) = \begin{cases} \dfrac{n^2}{sin^2(\psi_{FoV})} & 0 \le \psi \le \psi_{FoV} \\ 0 & \psi > \psi_{FoV} \end{cases} \quad (3)$$

Where ψ_{FoV} is the field of view for the receiver, and n is the refractive index. The optical power for the receiver is related to the channel, in our case is LOS, given in Eq. 2 and P_t is the transmitted power from the transmitter side. The received optical power given by (Matter et al., 2022):

$$P_r = H_{LoS}\,P_t \quad (4)$$

At the receiver side, SNR is considered to be evaluated on the receiver side. As the signal conveys to the receiver, it may be affected by noise. The SNR given by : (De Oliveira et al., 2022)

$$SNR = \frac{(RP_r)^2}{\sigma_{shot}^2 + \sigma_{thermal}^2} \quad (5)$$

Where R represents the responsivity of the photodiode at the receiver. Moreover, the signal transmission through a channel is affected by noise, shot noise, and thermal noise (De Oliveira et al., 2022). The shot noise is produced in the photodiode from background signal light, while thermal noise is related to electrons in the detector (Yin et al., 2021). The shot noise is given by (Chaurasia et al., 2020)

$$\sigma_{shot}^2 = 2qR\,P_rB + 2qI_2I_BB \quad (6)$$

and thermal noise given as (De Oliveira et al., 2022)

$$\sigma_{thermal}^2 = \frac{8\pi K T_k}{G} C A_r I_2 B^2 + \frac{16\pi^2 K T_k \eta}{g_m} C^2 {A_r}^2 I_3 B^3 \quad (7)$$

Where B is the bandwidth, Photocurrent is I_B, Noise bandwidth factors are I_2 and I_2, K is the Boltzmann constant, T_k the temperature, the open-loop voltage gain, denoted as G, the capacitance C of the detector, η is the noise factor of the channel and g_m is trans-conductance.
In the NLOS part, the signal reaches the receiver through additional paths because of reflections. In this model, we assumed a single reflection path where the signal is reflected through a small area in the wall or any reflection surface i, identified as A_{ref}, then reaches the receiver. The ray that reaches the reflector parts the angles into: the angle between the line from the transmitter to the, and the angle between the line from the reflector to the receiver is known β. The channel in this case is in the NLOS case, so modeled as (Poulose, 2022):

$$H_{NLoS} = \frac{(m+1)\,A}{2(\pi d_1 d_2)^2} \rho A_{ref} cos^m(\phi) \cos(\beta) \cos(\theta) T(\psi) g(\psi) \cos(\psi) \quad (8)$$

Where d_1 and d_2 are the distance form transmitter to the reflector and from the reflector to the receiver, respectively. ρ represents the reflectance factor. The received power in this case, where the path is considered from the first reflection, is given as (Poulose, 2022):

$$P_r = H_{NLoS} P_t \quad (9)$$

3 Simulation Results

The section presents simulation results for the system shown in Figure 1. The simulation result considers two cases: LOS simulation and NLOS simulation. In the first section, the simulation is evaluated to capture the effect of LOS and NLOS on the system with respect to various parameters from the transmitter side. In addition, to focus on system sensitivity against physical parameters on the receiver side, the LOS model was only considered.

3.1 LOS simulation results

The result offers the variation of the received power and SNR according to various parameters from the transmitter and receiver side in the case of a LOS channel. MATLAB program is used to perform the simulations. The simulation parameter used in this model is presented in Table 1.

Table 1: Simulation parameter

Parameter	Value
A	1 cm^2
$\boldsymbol{\varphi_{1/2}}$	70
n	1.5
$\boldsymbol{I_2}$	0.562
$\boldsymbol{I_3}$	0.0868
q	1.602e-19 c
R	0.5
$\boldsymbol{I_B}$	5.1 mA
K	1.38e-23
$\boldsymbol{T_k}$	300 k
$\boldsymbol{g_m}$	30×10^{-3} S
$\boldsymbol{G}$	10
C	12 p F/cm^2
B	10 MHz
$\boldsymbol{\eta}$	1.5

The simulation results in Figures 2 and 3 describe the variation of P_r as a function of distance for multiple values of transmitting angle for $m = 0.8\ and\ m = 3$, respectively. From Figure 2, the overall P_r exhibits a clear decrease with increasing distance, indicating the attenuation effect of distance. At shorter distances, noticeable differences among the curves are observed, suggesting that the irradiance angles have a significant impact on P_r in this region. However, as the distance increases, the curves gradually converge, implying that the influence of these parameters diminishes at larger distances.

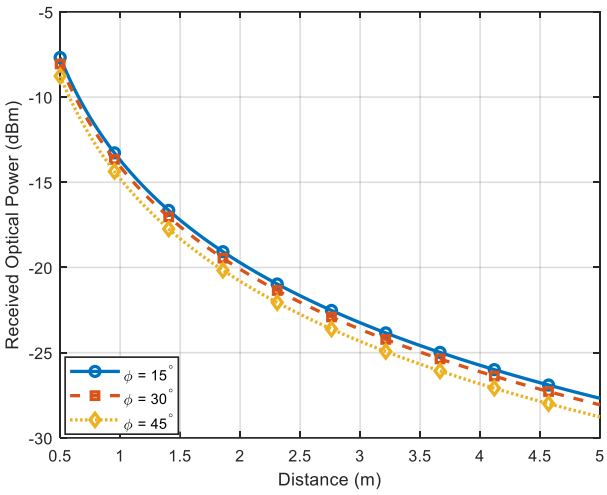

Figure 2: Received power vs distance for different ϕ with $m = 0.8$

This behavior demonstrates the strength of the system performance in the large distance region while highlighting the sensitivity of P_r to system parameters in the small distance region. In Figure 3, the received

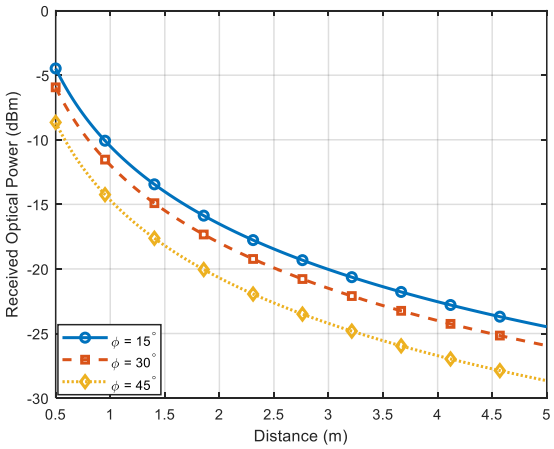

Figure 3: Received power vs distance for different ϕ with $m = 3$

power with distance for different values of ϕ I simulated for the case when the Lambertian order increases to 3, by comparison with the case when d = 1 and ϕ = 15, the received power changed from -14 dBm when m = 0.8 in Figure 2 to -10 dBm for m =3 in Figure 3. These results provide useful insights into the distance and angle-dependent features of the received power. Also, indicate the importance of the Lambertian order on the system performance.

Furthermore, the indirect effect of angle variation from the transmitter side is evaluated on SNR in the figures below. From Figure 4 (a), the results show the effect of the parameter **m** on the SNR performance over the variable of ϕ and distance. At low m value, m = 0.8, in this case, the maximum value for SNR is at the high edge when both ϕ and distance are small which is equal to ≈ 55 dB this value gradually decreases with increase in distance, also a low reduction caused by increasing in ϕ value because the power radiation in this model is

considered Lambertian pattern that relay on cosine law. As the Lambertian order increases to m =3 in Figure 4 (b) the value of maximum SNR is increased to 61 dB because **m** represents the intensity of the light beam as it increases, causing an increase in the SNR in a more concentrated region. This indicates the high sensitivity of the system performance to the variation in the Lambertian order parameter.

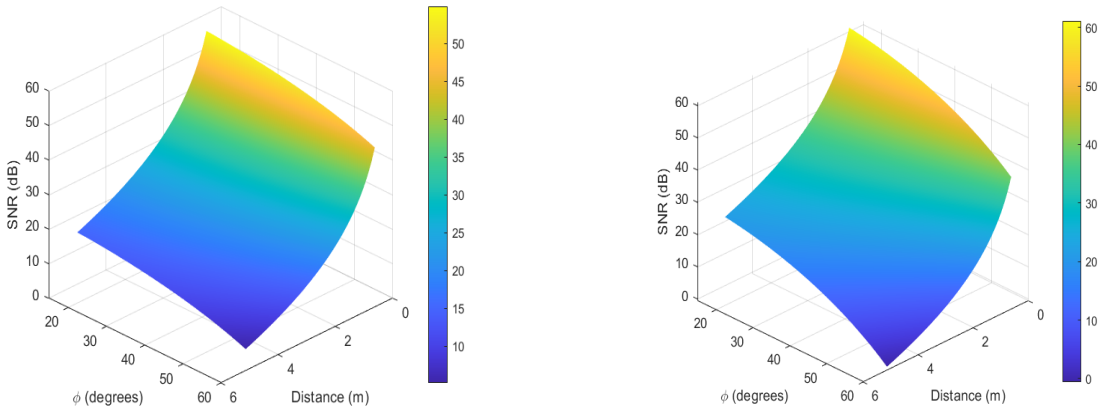

(a) (b)

Figure 4: SNR variation as a function of distance and ϕ when (a) m = 0.8 (a) m = 3

From the receiver side, we consider the LOS path only in simulation to focus on the sensitivity of the system for the concentrator gain and optical filter. The simulation results in Figure 5 (a) illustrate the variation of the received power as a function of the distance for several values of concentrator gain. The simulations show that as the concentrator gain rises significantly, leading to a much higher received power, especially at low distances. This is because the concentrator is focusing the accepted light onto the receiver. In contrast, as distance increases, the received power gradually decreases. For distance impact, P_r displays a clear decrease with increasing distance, demonstrating the attenuation effect of it. At shorter distances, clear variations among the curves of different gain values are observed, presenting that the gain effect has a significant influence on P_r in this region. Though as the distance increases, the curves converge, indicating that the impact of these parameters reduces at greater distances. Figure 5 (a) and (b) show these results in the case of optical filter value T = 1. Figure 5 (b) shows that the intensity variations are further distinct. In particular, regions of low and high power can clearly be identified. The hot spot means high values of P_r, while moderate to low values present color gradients, as the distance increases, the effect of distance rises, causing a decrease in the values of the received power, represented in a cold color region. The counterplot in Figure 5 (b) provides conception validation to the interpretation of the results.

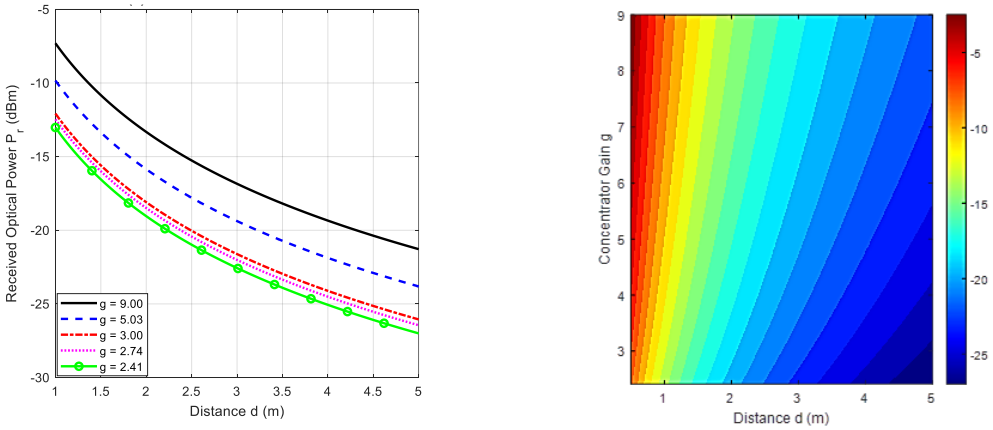

(a) (b)

Figure 5: P_r vs distance (a) as a function of concentrator gain (b) Contour plot when T = 1

Figure 6 (a) and (b) show the effect of optical filter variation on the performance. In Figure 6 (a) the simulation shows the decrease in the received power values as the filter value decreases from T =1 in Figure 5 (a) to T = 0.5, leading to a decrease in the received power from -10.9 dBm in Figure 5 (a) when g =9 and d =1.5 m to -14 dBm in Figure 6 (a). The optical filter works on filtering noise, and any unnecessary signals tend to enter the receiver, as its value change leads to high protection to the receiver side from incoming signals, thus may cause even reduction in the effective received power, so this trend is essential in system design. From Figure 6 (b) a significant insight into the number of hot spots of the P_r is shown. The hot spot regions (related to high power values in the whole system) is changed from -5 dBm in Figure 5 (b) when T = 1 to -10 dBm in Figure 6 (b) when T =0.5. This is almost equivalent to 3.16 in linear power scale, that mean received power at Figure 5 (b) is three times stronger than Figure 6 (b).

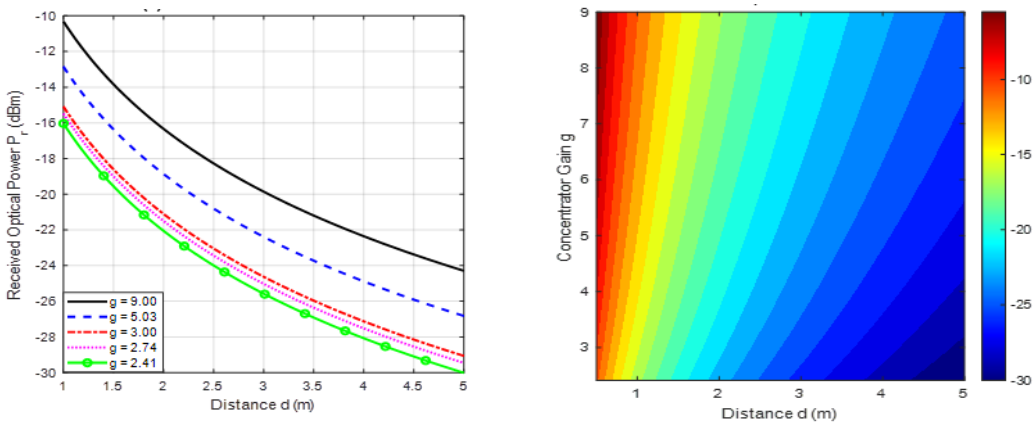

(a) (b)

Figure 6: P_r vs distance (a) as a function of concentrator gain (b) Contour plot when T = 0.5

Furthermore, the effect of the concentrator gains and distance on SNR is discussed in the following figures. The impacts of the concentrator gain and optical filter when T = 1 are presented in Figure 7 (a) and in a contour plot in Figure 7 (b), respectively. From the simulation in Figure 7 (a) the maximum value of SNR is 52 dB when **g** = 9 and d = 1.5 m, this value gradually decreases as the concentrator gain decreases and gets even lower values with increasing distances. This can be more recognized in Figure 7 (b) where the hot color region is focused on the range when the SNR is at the maximum level at specific range values of **g** and the distance.

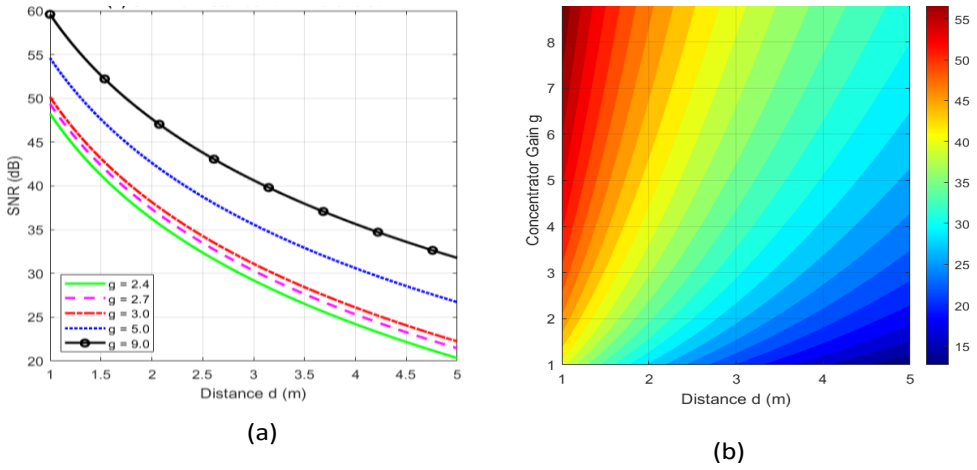

(a) (b)

Figure 7: SNR vs distance (a) as a function of concentrator gain (b) Contour plot when T = 1

In Figure 8, the SNR versus the distance is simulated as the value of the optical filter is adjusted to be 0.5 to show its effect on SNR. As seen in Figure 8 (a), the value of SNR decreases to 46 dB compared to Figure 7 (a) when g = 9 and d = 1.5 m. This presents how SNR is affected by the optical filter. Furthermore, Figure 8 (b) validates this effect on SNR, which shows the range of maximum SNR under T = 0.5 with the specific values of concentrator gain and distances.

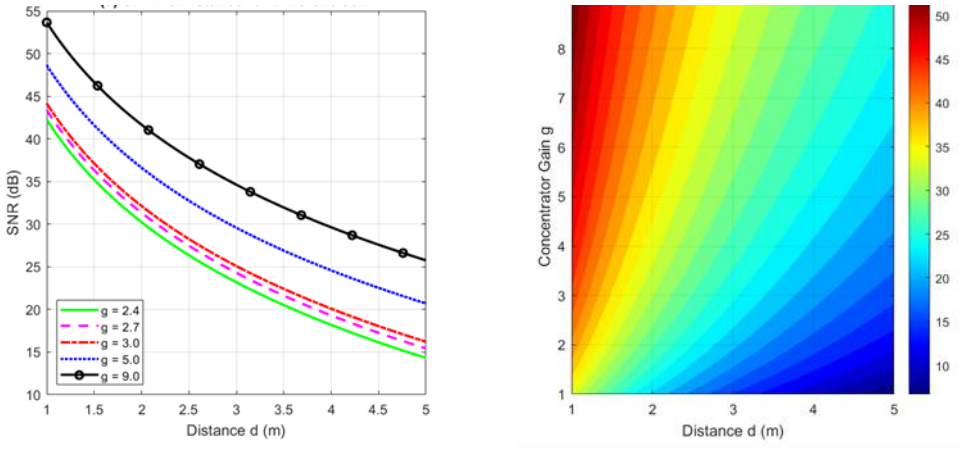

(a) (b)

Figure 8: SNR vs distance (a) as a function of concentrator gain (b) Contour plot when T = 0.5

3.2 NLOS simulation results

For NLOS in this case, the received power and SNR are evaluated. As presented in Figure 1, the path of the signal is not directly connected to the receiver is reflect then reaches the receiver. In our model, the first reflection of the signal is assumed. The specialized parameters used in this simulation are presented in Table 2.

Tabel 2: Simulation parameters value for NLOS

Parameter	Value
A_{ref}	1 cm^2
$\boldsymbol{\beta}$	1.5
$\boldsymbol{\theta}$	0.562
C	12 p F/cm^2

As shown in Figure 9, the figure represents the variation of the received power with distance for different values of ϕ. From the simulation noticed that the receiver power is reduced in NLOS compared to the LOS case in the previous section, and P_r drops faster as the distance increases compared to the LOS model in Figures 2 and 3. This sharp reduction is due to the reflected path of the signal.

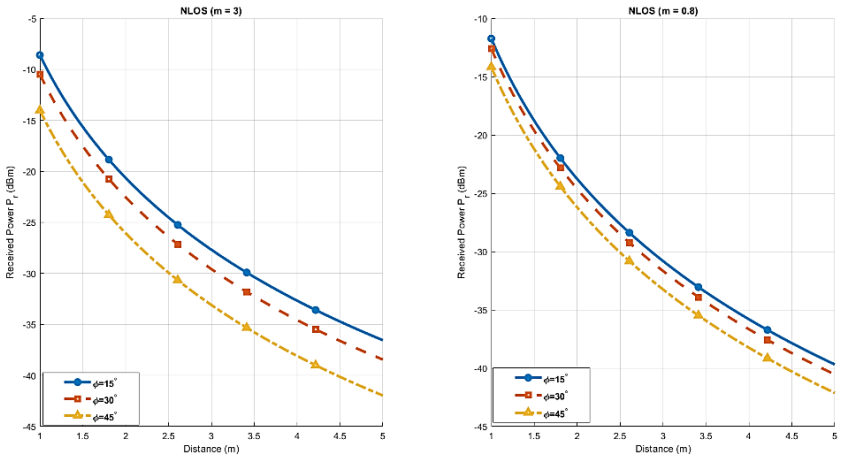

Figure 9: Received power vs distance for different ϕ with (a) $m = 3$ and (b) $m = 0.8$

As for the SNR simulation presented in Figure 10 (a), compared to Figure 4 (a) where m = 0.8, the maximum value evaluated is 55 dB, while in NLOS, the value is reduced to 53. These comparisons were evaluated when the SNR was evaluated at a small distance. As the distances increase, the reduction in NLOS is higher, causing negative SNR values. While in Figure 10 (b) when m increased to 3 the maximum SNR increased to 60, compared to Figure 10 (a) show the critical role of this parameter on the system performance even in an NLOS environment.

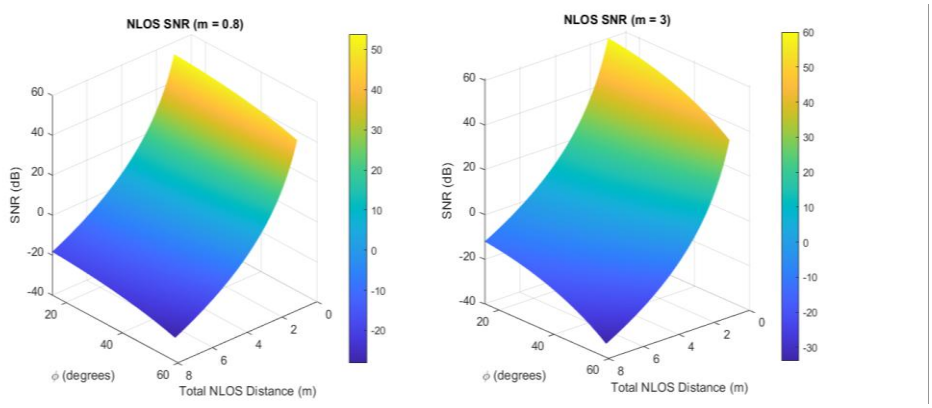

Figure 10: SNR variation vs distance and ϕ for (a) $m = 0.8$ and (b) $m = 3$

4 Conclusion

In this paper, the performance of VLC under the incorporation of the distance and the transmitted angle on the received power and SNR from the transmitter side in LOS and NLOS is presented. In the LOS model, simulation results show that the transmitted angle influences the received power, causing a reduction in its value, particularly in small distance values; furthermore, for the SNR maximum value evaluated to be almost 55 dB at low distances and small irradiance angles, and a slight reduction is evaluated as the irradiance angle increases. In addition, the performance undergoes a reduction in received power and SNR in an NLOS environment, especially at large distances. From the receiver side, the effect of distance and concentrator gain on receiver power is studied for different optical filter values. The results show that a high value for concentrator gain provides a high level of received power, -6 dBm, with an optical filter equal to T = 1. An optical filter is used on the receiver side, causing a reduction in the amount of the received power and SNR .

Authors Contribution

The corresponding author conducted all aspects of the research.

Data Availability

The data that support this study are available from the corresponding author upon request

Conflict of Interests

The authors declare that there are no conflicts of interest regarding the publication of this manuscript

Funding

No external funding support was received for this study.

References

Abdalla, I., Rahaim, M. B., & Little, T. D. (2020). On the importance of dynamic FOV receivers for dense indoor optical wireless networks. ICC 2020-2020 IEEE International Conference on Communications (ICC), https://doi.org/10.1109/ICC40277.2020.9149050.

Abualhoul, M. Y., Marouf, M., Shag, O., & Nashashibi, F. (2014). Enhancing the field of view limitation of visible light communication-based platoon. 2014 IEEE 6th International Symposium on Wireless Vehicular Communications (WiVeC 2014), https://doi.org/10.1109/WIVEC.2014.6953221.

Al-Sakkaf, A. G. A., & Morales-Céspedes, M. (2024). Interference management for VLC indoor systems based on overlapping field-of-view angle diversity receivers. *IEEE Access*, *12*, 51431-51449, https://doi.org/10.1109/ACCESS.2024.3381968.

Al Hasnawi, R., Marghescu, C. I., & Rusu-Casandra, A. (2025). Enhancing vehicular VLC systems with multi-relay techniques: a performance evaluation. *Electronics*, *14*(6), 1170. https://doi.org/10.3390/electronics14061170

Antaki, B., Dalloul, A. H., & Miramirkhani, F. (2025). Intelligent health monitoring in 6g networks: Machine learning-enhanced vlc-based medical body sensor networks. *Sensors*, *25*(11), 3280. https://doi.org/10.3390/s25113280

Ariyanti, S., & Suryanegara, M. (2020). Visible light communication (VLC) for 6G technology: The potency and research challenges. 2020 Fourth world conference on smart trends in systems, security and sustainability (WorldS4), https:// doi.org/10.1109/WorldS450073.2020.9210383.

Batista, A. A., Amorim, T. D., Ribeiro, R. M., Barbero, A. P., Di Renna, R. B., Peixoto, F. C., & Silva, V. N. (2025). Enhanced Photodetector Field of View for IoT-Driven VLC Systems Using Fluorescent Optical Antennas. *IEEE Access*. https://doi.org/10.1109/access.2025.3593261.

Chaurasia, A., Sharma, M., Akansha, Garg, A., & Rani, R. (2020). Statistical analysis of SNR and optical power distribution in an indoor VLC System. Journal of Physics: Conference Series, https://doi.org/10.1088/1742-6596/1706/1/012067.

Chowdhury, M. Z., Joha, M. I., Rahman, M. M., Kabir, M. S., & Jang, Y. M. (2025). Machine learning and deep learning in VLC systems: A comprehensive survey. *IEEE Open Journal of the Communications Society*. https:// doi.org/ 10.1109/OJCOMS.2025.3603200.

De Oliveira, M., Tosta, F. C. B., Guillen, D. E. F., Monteiro, P. P., & Pohl, A. d. A. P. (2022). Theoretical and experimental analysis of LED lamp for visible light communications. *Wireless Personal Communications*, *125*(4), 3461-3477. https://doi.org/10.1007/s11277-022-09720-z.

Ding, J., Chih-Lin, I., Chen, X., & Lai, H. (2019). Asymmetrical emission beams based visible light communication access points design. 2019 28th Wireless and Optical Communications Conference (WOCC), https://doi.org/10.1109/WOCC.2019.8770572

Eroğlu, Y. S., Yapıcı, Y., & Güvenç, I. (2018). Impact of random receiver orientation on visible light communications channel. *IEEE Transactions on Communications*, *67*(2), 1313-1325. https:// doi.org/ 10.1109/TCOMM.2018.2879093.

Eso, E., Ghassemlooy, Z., Zvanovec, S., Pesek, P., & Sathian, J. (2021). Vehicle-to-vehicle relay-assisted VLC with misalignment induced azimuth or elevation offset angles. *IEEE Photonics Technology Letters*, *33*(16), 908-911. https://doi.org/10.1109/LPT.2021.3086836.

Farfán–Guillén, D. E., Junior, P. D. T. N., & Pohl, A. D. A. P. (2021). Performance evaluation of a LoS visible light communication link using an optical concentrator and a plano-convex lens. In *Proceedings of the 2021 Third South American Colloquium on Visible Light Communications (SACVLC)*, https://doi.org/10.1109/SACVLC53127.2021.9652389.

He, C., & Chen, C. (2023). A review of advanced transceiver technologies in visible light communications. *Photonics, 10*(6), Article 648. https://doi.org/10.3390/photonics10060648.

Jaque Intriago, N., Cueva Ayala, A., Aguirre Navas, C., Taipe Chicaiza, W., & Paredes-Paredes, M. C. (2025). Performance Analysis of DCO-OFDM in IEEE 802.11 bb VLC PHY Modes: Impact of Biasing Techniques and Optical Channel Dispersion. *Engineering Proceedings*, *115*(1), 21. https://doi.org/10.3390/engproc2025115021

Jayaweera, V. L., Peiris, C., Darshani, D., Edirisinghe, S., Dharmaweera, N., & Wijewardhana, U. (2025). Visible light communication for underwater applications: Principles, challenges, and future prospects. *Photonics,* https://doi.org/10.3390/photonics12060593.

Matter, K. M., Fayed, H. A., El-Aziz, A. A., & Aly, M. H. (2022). Enhanced bit error rate in visible light communication: a new LED hexagonal array distribution. *Optical and Quantum Electronics*, *54*(8), 506. https://doi.org/10.1007/s11082-022-03889-0.

Nagaraja, K., Dash, S. P., & Ghose, D. (2025). Channel Estimation and Error Analysis of a Narrow FoV VLC System With Random Receiver Orientation. *IEEE Open Journal of the Communications Society*. https://doi.org/10.1109/OJCOMS.2025.3557522.

Poulose, A. (2022). Simulation of an indoor visible light communication system using optisystem. *Signals*, *3*(4), 765-793. https://doi.org/10.3390/signals3040046.

Putri, N. A. Y., Hambali, A., & Pamukti, B. (2019). VLC system performance evaluation with addition of optical concentrator on photodetector. *In Proceedings of the 2019 IEEE International Conference on Signals and Systems (ICSigSys). IEEE.* https://doi.org/10.1109/ICSIGSYS.2019.8811069.

Raj, R., Jaiswal, S., & Dixit, A. (2020). On the effect of multipath reflections in indoor visible light communication links: Channel characterization and BER analysis. *IEEE Access*, *8*, 190620-190636. https://doi.org/10.1109/ACCESS.2020.3031164

Saxena, K., Raj, R., & Dixit, A. (2018). A novel optimization approach for transmitter semi-angle and multiple transmitter configurations in indoor visible light communication links. In *Proceedings of the 2018 9th International Conference on Computing, Communication and Networking Technologies (ICCCNT)*, https://doi.org/10.1109/ICCCNT.2018.8493666.

Yin, Y., Tang, P., Liu, B., Zhang, J., Xia, L., & Liu, B. (2021). The comparison and analysis of different noise models for visible light communication. In *Proceedings of the International Conference on Frontiers of Electronics, Information and ComputationTechnologies*. ACM. https://doi.org/10.1145/3474198.3478224.

Zhou, G., Papanikolaou, V. K., Ding, Z., & Schober, R. (2025). Channel estimation for mmWave pinching-antenna systems. In *Proceedings of the 2025 IEEE 26th International Workshop on Signal Processing and Artificial Intelligence for WirelessCommunications(SPAWC)*. https://doi.org/10.1109/SPAWC66079.2025.11143413.